Quantum Information Processing (2019) 18:41
https://doi.org/10.1007/s11128-018-2157-6

Entanglement generation between distant parties via disordered spin chains

Guilherme M. A. Almeida[1] · Francisco A. B. F. de Moura[1] · Marcelo L. Lyra[1]

Received: 30 May 2018 / Accepted: 15 December 2018
© Springer Science+Business Media, LLC, part of Springer Nature 2019

Abstract
We study the emergence of bipartite entanglement between a pair of spins weakly connected to the ends of a linear disordered XY spin-1/2 channel. We analyze how their concurrence responds to structural and on-site fluctuations embodied by long-range spatially-correlated sequences. We show that the end-to-end entanglement is very robust against disorder and asymmetries in the channel provided that the degree of correlations are strong enough and both entangling parties are tuned accordingly. Our results offer further alternatives in the design of stable quantum communication protocols via imperfect spin channels.

Keywords Quantum entanglement · Anderson localization · Quantum state transfer

1 Introduction

Transmitting quantum states and establishing entanglement between different quantum processing units are essential ingredients toward the implementation of large-scale quantum computing [1]. In this context, a promising approach relies on using solid-state devices such as spin chains with pre-engineered interactions as quantum channels [2] for quantum communication protocols. In such, the information is usually encoded locally and after proper channel initialization and subsequent time evolution, the initial state (say, a qubit) can be retrieved at the desired location, or entanglement can be created during the process. The key point is to devise the protocols whose working principle is based solely upon *how* the chain is engineered, avoiding the need of external control as much as possible. After the overall concept was put forward by Bose in Ref. [2], much effort has been devoted to find out further schemes for performing quantum state transfer (QST) [3–15] and entanglement creation/distribution protocols [16–21].

✉ Guilherme M. A. Almeida
gmaalmeidaphys@gmail.com

[1] Instituto de Física, Universidade Federal de Alagoas, Maceió, AL 57072-900, Brazil

Published online: 01 January 2019

The versatility offered by spin chains comes with a price though. The lack of dynamical control implies that the manufacturing process of the chain must be very accurate [22,23]. Otherwise, the appearance of imperfections (e.g., disorder) should compromise the desired output. There lies the importance of evaluating the robustness of such quantum communication protocols in the presence of noise [21,24–31].

Here, we go along that direction and address the influence of disorder in weakly coupled spin models [5–7]. In the QST framework, a pair of spins are perturbatively connected to, say, each end of a XY spin-1/2 chain thereby spanning a decoupled Hamiltonian involving both spins only or added with a given normal mode of the channel once their frequency goes in resonance with it [6]. Ideally, that is, in a noiseless channel, this decoupling process yields the appearance of maximally entangled Bell-type eigenstates which are responsible for Rabi-like oscillations between the sender and receiver spins thus allowing for high-fidelity QST performances [13]. Random fluctuations, on the other hand, will act on the channel by shuffling the spectrum, promoting localization, and destroying the mirror symmetry of every eigenstate in the system [28].

When correlated fluctuations—say, spatially dependent—are present the scenario is rather different. For instance, it was shown that short-range correlations in the disorder distribution promotes the breakdown of Anderson localization in 1D models [32]. The effect of long-range correlations is even more dramatic as it induces a metal–insulator transition with sharp mobility edges [33,34]. The coexistence between localized and delocalized states hence provides a rich set of dynamical regimes to explore [34–36].

Properties and dynamics of entanglement in disordered spin chains have attracted a great deal of interest in the past few years [26,37,38]. In [39–41], the scaling behavior of the ground-state entanglement entropy of a spin block was studied for certain types of correlated random critical chains. It was shown that disorder may improve the amount of entanglement shared by the subsystems (see [39]). From the quantum networking perspective, it was found that many classes of weakly coupled spin models support the existence of long-distance entanglement in its ground state [18,19,42] (see [43] for a recent experimental realization) which in turn can serve as a resource for quantum teleportation protocols. Its resilience against static disorder was investigated in detail in [42]. There, it was evaluated that the entanglement quality depends upon the intensity of disorder, as expected. In some cases though, imperfections may not be detrimental to the system. Local defects, for instance, can be harnessed to control and enhance entanglement on demand [17,44]. Quite recently, it has been reported that the emergence of long-range-correlated fluctuations in the local magnetic fields is capable of modifying the entanglement distribution profile in XY spin chains [21].

In this work, we investigate how correlated diagonal (local magnetic fields) and off-diagonal (spin couplings) disorder affect the stability of the eigenstate entanglement developed from both end spins perturbatively coupled to the noisy channel, in the single-excitation manifold. We consider fluctuations which follow a power-law spectrum of the form $S(k) \propto 1/k^{\alpha}$, with k being the corresponding wave number and α is an exponent that characterizes the *degree* of those correlations with $\alpha = 0$ standing for the uncorrelated case. For high-enough values of α we find that the end-to-end concurrence reaches about its maximum value despite the fact that significant amounts of disorder are still present. We further discuss what kind of profile a given

channel must have in order to mediate entanglement in the presence of imperfections. The emergence of a set of delocalized states in the middle of the spectrum when $\alpha > 2$ [33] becomes crucial in generating an effective resonant coupling between both distant parties. Our findings settle a resilient framework for carrying out long-distance quantum communication protocols through highly disordered quantum channels.

2 Hamiltonian

Throughout the paper, we consider a one-dimensional isotropic XY spin-1/2 chain with open boundaries featuring $N+2$ spins labeled by $i = 0, 1, 2, \ldots, N, N+1$, with spins 0 and $N+1$ denoting the parties aimed to get entangled. The full Hamiltonian of the system reads ($\hbar = 1$)

$$\hat{H} = \sum_{i=0}^{N+1} \frac{\omega_i}{2}(\hat{1} - \hat{\sigma}_i^z) - \sum_{i=0}^{N} \frac{J_i}{2}(\hat{\sigma}_i^x \hat{\sigma}_{i+1}^x + \hat{\sigma}_i^y \hat{\sigma}_{i+1}^y), \tag{1}$$

where $\hat{\sigma}_i^{x,y,z}$ comprise the Pauli operators for the ith spin, ω_i is the local magnetic field, and J_i is the nearest-neighbor exchange coupling rate (all those being real parameters). For simplicity, we set the above Hamiltonian to be expressed in terms of an arbitrary energy unit $J = 1$. Hereafter, we relabel $0 \to s$ and $N+1 \to r$ and assume those to be weakly coupled to each end of the channel, hence fixing $J_0 \to g_s$ and $J_N \to g_r$, both being much smaller than any other J_i, and free of imperfections alongside ω_s and ω_r. Therefore, we consider disorder to take place in the channel only (that is, from spins 1 to N). This is a reasonable assumption in the sense that spins s and r are the only components of the system supposed to feature a higher degree of control due to the need of performing state preparation and read-out protocols on them. We will specify the disorder distribution later on.

Note that $\left[\hat{H}, \sum_i \hat{\sigma}_i^z\right] = 0$ and hence Hamiltonian (1) is made up by independent blocks with fixed number of excitations. In standard QST protocols [2], one wishes to transmit the state of a single qubit through an initially polarized channel such that $|\Psi(0)\rangle = |\phi\rangle_s|\downarrow_1, \ldots, \downarrow_N, \downarrow_r\rangle$ with $|\phi\rangle_s = a|\downarrow_s\rangle + b|\uparrow_s\rangle$. The goal is to achieve $|\Psi(t)\rangle = |\downarrow_s, \downarrow_1, \ldots, \downarrow_N\rangle|\phi\rangle_r$ in a given time t. The whole process takes place in subspaces with none and single flipped spins, the latter being the only component which actually evolves in time. We thus carry out our investigation on the subspace spanned by $|i\rangle \equiv |\downarrow_s, \downarrow_1, \downarrow_2, \ldots, \downarrow_{i-1}, \uparrow_i, \downarrow_{i+1}, \ldots, \downarrow_r\rangle$.

In this work, we consider the presence of *static* disorder in the channel, taking place either in the local magnetic fields or in the spin couplings. We model that by sequences featuring long-range correlations following a power-law spectrum of the form $S(k) \propto 1/k^\alpha$ as generated from [33,34]

$$\omega_n, J_n = \sum_{k=1}^{N/2} k^{-\alpha/2} \cos\left(\frac{2\pi nk}{N} + \phi_k\right), \tag{2}$$

where $n = 1, \ldots, N$, $\{\phi_k\}$ are random phases uniformly distributed in the interval $[0, 2\pi]$ and α stands for the degree of those underlying correlations. We remark that the above distribution possess no typical length scale, as does many natural stochastic series [45]. Uncorrelated disorder, i.e., white noise, is recovered when $\alpha = 0$. Indeed, α is directly related to the so-called Hurst exponent H [46] through $H = (\alpha - 1)/2$ which characterizes self-similarity of a given series. The sequence spanned by Eq. (2) becomes nonstationary when $\alpha > 1$ and is said to be persistent (anti-persistent) when $\alpha > 2$ ($\alpha < 2$). The $\alpha = 2$ case is where the sequence corresponds exactly to the trace of the Brownian motion. In our calculations, we set the disorder sequence to have zero mean and unit variance, $X_n \to (X_n - \langle X_n \rangle) / \sqrt{\langle X_n^2 \rangle - \langle X_n \rangle^2}$, with X_n representing any stochastic variable. When considering disorder in the spin couplings, we also recast $J_n \to J_n + 4.5$. This is done to make all the couplings positive so that the ground state is ferromagnetic. Also, the weak-coupling regime implies that the outer couplings $g/J_n \ll 1$. Thereby, in order to keep g about the same order of magnitude in each diagonal (for which $J_n \equiv 1$) and off-diagonal disorder configurations, it turns out to be necessary to shift $\langle J_n \rangle$ away from zero.

3 Perturbation theory

Now, we proceed by carrying out a perturbative approach in order to find an equivalent Hamiltonian that effectively couple the sender/receiver pair of spins. To do so, we go along the procedure used in Ref. [6]. The first step is to diagonalize Hamiltonian (1) in the channel sector (comprising states $|1\rangle$ through $|N\rangle$), thus obtaining the channel normal modes $\{|E_k\rangle\}$ and their associated frequencies $\{E_k\}$, which we assume to be nondegenerate (we do not need to worry about their exact form at this point). Wiring up spins s and r to the channel we express the full Hamiltonian in a very convenient form $\hat{H} = \hat{H}_0 + \hat{V}$, where

$$\hat{H}_0 = \omega_s |s\rangle\langle s| + \omega_r |r\rangle\langle r| + \sum_k E_k |E_k\rangle\langle E_k|, \tag{3}$$

$$\hat{V} = \epsilon \sum_k \left(g_s a_{sk} |s\rangle\langle E_k| + g_r a_{rk} |r\rangle\langle E_k| + \text{H.c.} \right), \tag{4}$$

with $a_{sk} \equiv \langle 1|E_k\rangle$, and $a_{rk} \equiv \langle N|E_k\rangle$ being real-valued coefficients. Note that we have introduced a perturbation parameter ϵ in order to assure that spins r and s do not disturb the band. Therein, we highlight two possibilities, namely (i) both spins are out of resonance with all the normal modes of the channel, or (ii) they eventually meet one of those such that $\omega_s = \omega_r = E_{k'}$. Let us treat each case separately.

In the first scenario (i), we define $\hat{H}_{\text{eff}} = e^{i\hat{S}} \hat{H} e^{-i\hat{S}}$ with $\hat{S}$ being a Hermitian operator with entries $\langle \nu|\hat{S}|E_k\rangle = i\epsilon g_\nu a_{\nu k}/(E_k - \omega_\nu)$, where $\nu \in \{s, r\}$ (see [6,7]). Expanding $\hat{H}_{\text{eff}}$ up to second order in ϵ we get

$$\hat{H}_{\text{eff}} = \hat{H}_0 + \hat{V} + i[\hat{S}, \hat{H}_0] + i[\hat{S}, \hat{V}] + \frac{i^2}{2!}[\hat{S}, [\hat{S}, \hat{H}_0]] + O(\epsilon^3). \tag{5}$$

Due to the choice of $\hat{S}$, the first-order terms in the above expression vanish, $\hat{V} + i[\hat{S}, \hat{H}_0] = 0$. Then, by inspecting Eq. (5), we now have $\hat{H}_{\text{eff}} = \hat{H}_{sr} \oplus \hat{H}_{\text{ch}}$, where [6]

$$\hat{H}_{sr} = h_s|s\rangle\langle s| + h_r|r\rangle\langle r| - J'\left(|s\rangle\langle r| + \text{H.c.}\right), \tag{6}$$

thus describing a two-level system with effective local potentials and coupling given by, respectively,

$$h_v = \omega_v - \epsilon^2 g_v^2 \sum_k \frac{|a_{vk}|^2}{E_k - \omega_v}, \tag{7}$$

$$J' = \frac{\epsilon^2 g_s g_r}{2} \sum_k \left(\frac{a_{sk} a_{rk}}{E_k - \omega_s} + \frac{a_{sk} a_{rk}}{E_k - \omega_r} \right). \tag{8}$$

At this point, we mention that the precise condition of validity for the above perturbative approach is $\epsilon g_{s,r} \ll |E_k - \omega_{s,r}|$. The eigenstates of Hamiltonian (6) can be easily handled out analytically, yielding

$$|\psi^{\pm}\rangle = \frac{2J'|s\rangle + (\Delta \pm \Omega)|r\rangle}{\sqrt{(\Delta \pm \Omega)^2 + 4J'^2}}, \tag{9}$$

where $\Delta \equiv h_s - h_r$ is the effective detuning and $\Omega = \sqrt{\Delta^2 + 4J'^2}$ is their corresponding Rabi-like frequency. In order to achieve a maximally entangled state, one then needs $\Delta = 0$ (or, at least, $|\Delta| \ll |J'|$) which results in $|\psi^{\pm}\rangle \sim (|s\rangle \pm |r\rangle)/\sqrt{2}$.

In case (ii) where both outer spins achieves resonance with a particular mode of the channel (say, labeled by k'), leaving the rest of the band untouched so that we can safely neglect off-resonant, fast-rotating interactions, an effective three-level Hamiltonian can be obtained [6],

$$\hat{H}_{sk'r} = \epsilon \left(g_s a_{sk'} |s\rangle\langle E_{k'}| + g_r a_{rk'} |r\rangle\langle E_{k'}| + \text{H.c.} \right), \tag{10}$$

where we have shifted the local frequencies (diagonal terms) $E_{k'} \to 0$ with no loss of generalization. Note that the above Hamiltonian is of first order in g, in contrast with the off-resonant regime which is of second order.

Hamiltonian (10) can be worked out exactly. Particularly, we are interested in the zero eigenstate $|\psi_0\rangle \equiv (d_1, d_2, d_3)$ which fulfills $\hat{H}_{sk'r}|\psi_0\rangle = 0$. Thereby, one must have $d_2 = 0$ (no component in $|E_{k'}\rangle$) and $d_1 g_s a_{sk'} + d_3 g_r a_{rk'} = 0$. After proper normalization, the eigenstate reads

$$|\psi_0\rangle = \frac{|s\rangle - \eta|r\rangle}{\sqrt{1 + \eta^2}}, \tag{11}$$

where $\eta \equiv g_s a_{sk'}/g_r a_{rk'}$ accounts for the balance between both effective couplings. Obviously, when $\eta = \pm 1$ the zero mode becomes fully entangled.

Note that up to now we have not made any specific assumptions toward the profile of the channel eigenstates so that the above formulas hold for any arbitrary network and provide us great insight about how the entanglement between the outer spins s and r depends upon the spectrum properties of the channel.

4 End-to-end concurrence

A powerful tool to quantify bipartite entanglement between two qubits in an arbitrary mixed state is the so-called concurrence [47]. Consider an arbitrary quantum state written on the computational basis, $|\psi\rangle = \sum_i d_i|i\rangle$, with d_i being, in general, a complex coefficient. The input information we need to proper characterize entanglement between a given pair of spins i and j is found in their corresponding reduced density matrix ρ_{ij} defined in basis $\{|\downarrow_i\downarrow_j\rangle, |\uparrow_i\downarrow_j\rangle, |\downarrow_i\uparrow_j\rangle, |\uparrow_i\uparrow_j\rangle\}$, which is obtained by tracing out all the remaining sites. Concurrence is then defined as $C(\rho_{ij}) = \max\{0, \sqrt{\lambda_1} - \sqrt{\lambda_2} - \sqrt{\lambda_3} - \sqrt{\lambda_4}\}$ [47], where $\{\lambda_i\}$ are the eigenvalues, in decreasing order, of the non-Hermitian matrix $\rho_{ij}\tilde{\rho}_{ij}$, with $\tilde{\rho}_{ij} = (\hat{\sigma}_y \otimes \hat{\sigma}_y)\rho^*_{ij}(\hat{\sigma}_y \otimes \hat{\sigma}_y)$. In the single-excitation manifold, the concurrence reads (for details, see [16])

$$C_{i,j} \equiv C(\rho_{ij}) = 2|d_i d_j^*|, \tag{12}$$

which gives $C_{i,j} = 0$ for non-entangled (separable) spins and $C_{i,j} = 1$ for maximally entangled parties.

By inspecting Eqs. (9) and (11) from the previous section, one gets

$$C^{(i)} \equiv C_{s,r} = \frac{2}{\sqrt{(\Delta/J')^2 + 4}}, \tag{13}$$

$$C^{(ii)} \equiv C_{s,r} = \frac{2|\eta|}{1 + \eta^2}, \tag{14}$$

for the effective two-level description given by H_{sr} [Eq. (6)] for the three-level regime expressed by $H_{sk'r}$ [Eq. (10)], respectively. Therefore, we verify that the quality of entanglement between spins s and r will be ultimately dictated by the quantities Δ/J' or η, depending on the interaction regime we are dealing with. Setting $g_s = g_r$ and $\omega_s = \omega_r$, we note that for noiseless mirror-symmetric channels the conditions for maximal entanglement are readily fulfilled, since $|a_{sk}| = |a_{rk}|\ \forall\ k$, which gives $\Delta = 0$, $|\eta| = 1$, and thus $C_{s,r} = 1$.

Fluctuations in the parameters of the chain can then seriously damage the above (very suitable) scenario. Uncorrelated disorder ($\alpha = 0$) in 1D hopping models is known to induce the phenomenon Anderson localization [48] when every eigenstate of the system acquires the form $\langle x|E_k\rangle \sim e^{-\frac{|x-x_0|}{\xi_k}}$, thus becoming exponentially localized around a given position x_0 with ξ_k accounting for the localization length. As a consequence, it becomes extremely unlikely to find eigenstates $|E_k\rangle$ featuring comparable amplitudes a_{sk} and a_{rk} anywhere in the spectrum, given the length of the chain is much larger than the localization length. In principle, one could fight against

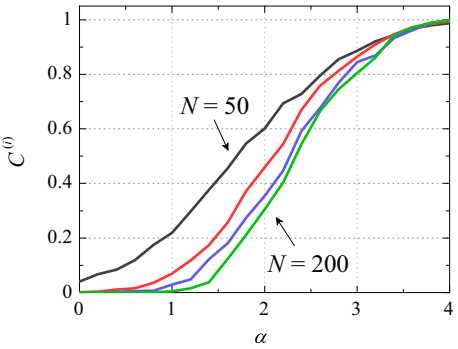

Fig. 1 End-to-end concurrence for the effective two-level case, $C^{(i)} = 2[(\Delta/J')^2 + 4]^{-1/2}$, versus α averaged over 500 independent realizations of on-site disorder for various channel sizes $N = 50$, 100, 150, and 200. We set $\omega_r = \omega_s = 0$, $g_s = g_r$ and $J_n/J = 1$. The input parameters of the channel, $a_{\nu k}$ and E_k, were obtained directly from exact numerical diagonalization of Hamiltonian (1) without the outer spins (Color online)

that by locally tuning either g_ν and/or ω_ν to compensate such distortion [28]. In the effective three-level regime described by $H_{sk'r}$, that should work well since all we need is $\eta = g_s a_{sk'}/g_r a_{rk'} \approx 1$ given a *fixed* frequency $E_{k'}$, otherwise we must also reset ω_ν to find another mode to tune with, for each disorder configuration. In the effective two-level case, though, the situation is more subtle. First of all, note that the ratio Δ/J does not depend upon a single channel eigenstate but on the entire spectrum [see Eqs. (7) and (8)] weighted by the inverse of the "distance" between E_k and ω_ν. In addition, in this case, there is no freedom in manipulating g_ν since it might lead to a mixing between the channel and sender/receiver subspaces, thus invalidating Hamiltonian (6). Despite all that, since there is no way to exactly predict a given disorder configuration, it should be much more preferable to fix ω_ν, g_ν and make sure that, statistically, the protocol yields successful outcomes up to a given user-defined threshold. This also rules out the need of additional resources.

5 Results and discussion

5.1 On-site disorder

We are now about to discuss the effects of long-range correlated disorder in the generation of entanglement. Let us start by considering noise on the local magnetic fields distribution $\{\omega_n\}$ [given by Eq. (2)] and fixing $J_n = 1$ (in units of J). Note that regardless of the parity of the chain size, disorder shuffles every natural frequency of the channel and so there will be no unique level to satisfy Hamiltonian (10). For this reason, in the case of on-site disorder, we only address the likelihood of entanglement taking place in the effective two-level scenario [Eq. (6)].

In Fig. 1, we show the resulting behavior of the disorder-averaged concurrence as a function of the degree of correlations α for different sizes of the channel, N. It starts off with a very poor figure of merit for lower values of α, as expected, and

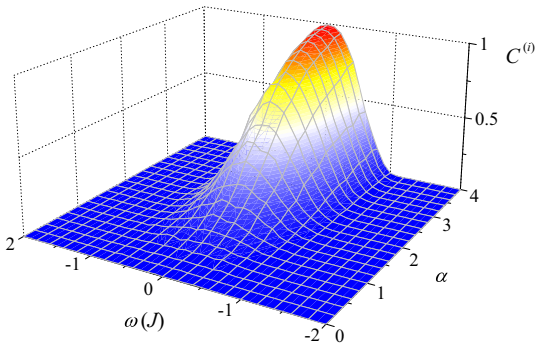

Fig. 2 End-to-end concurrence for the effective two-level case, $C^{(i)} = 2[(\Delta/J')^2 + 4]^{-1/2}$, for varying α and frequency $\omega = \omega_r = \omega_s$ averaged over 500 independent realizations of on-site disorder for $N = 100$, $g_s = g_r$, and $J_n/J = 1$. Therein, we certify that maximal entanglement can only be achieved when tuning spins s and r around the center of the band. For the range of α considered here, the bandwidth goes from about $-3.5J$ to $3.5J$ (Color online)

reaches about its maximum, $C^{(i)} \approx 1$, when $\alpha = 4$. As N increases—thus weakening finite-size effects—we also note that the concurrence begins to suddenly build up after $\alpha = 1$. This is related to the fact that the series generated by Eq. (2) becomes nonstationary, preceding the appearance of a set of delocalized states around the center of the band, induced by the persistent character of the series when $\alpha > 2$ [33]. This region of the spectrum thus offers a suitable ground for creating entanglement since the corresponding channel eigenstates $\{|E_k\rangle\}$ are expected to feature more balance between a_{sk} and a_{rk}, this way increasing the possibilities of having $|\Delta/J'| \ll 1$. The outer parts of the band, still composed by strongly-localized modes, have a much weaker influence on that since the terms inside the sum in Eqs. (7) and (8) decreases following E_k^{-1}. Because of that, the sender/receiver local frequencies must be set as close as possible to the center of the band (as in Fig. 1). If they do not, Fig. 2 shows exactly what happens. As we shift $\omega = \omega_s = \omega_r$ away from 0, the concurrence drops very rapidly since the effective coupling between both spins becomes more sensitive to the imperfections and asymmetries of the channel.

It is worth mentioning that for a fully uniform (ordered) channel, the concurrence would be maximum, in the weak-coupling limit, for the entire range of ω as long as it does not match any of the channel natural frequencies E_k so as to secure the off-resonant, two-level regime. In this particular case, we always have $\Delta = 0$ and a finite J' that gets extremely small as $|\omega| \ll |2J|$ (the bandwidth of a uniform channel goes from $-2J$ to $2J$). The above situation is very different from that involving correlated disorder where set of (asymmetric) delocalized states is only available around the middle of the band.

5.2 Coupling disorder

Now let us move on to the case of structural disorder, i.e., fluctuations affecting the spin-coupling strengths of the channel, $\{J_n\}$. First, we must have in mind that this kind

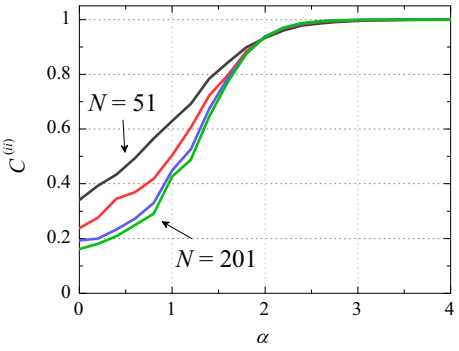

Fig. 3 End-to-end concurrence for the effective three-level regime, $C^{(ii)} = 2|\eta|(1+\eta^2)^{-1}$, versus α averaged over 500 independent realizations of spin-coupling strength disorder for various channel sizes $N =$ 51, 101, 151, and 201. We set $\omega_s = \omega_r = 0$ (matching the central anomalous mode), $g_s = g_r$, and $\omega_n = 0$ (channel local magnetic fields) (Color online)

of disorder, despite breaking the spatial mirror symmetry of the system, it preserves particle–hole symmetry meaning that $E_k = -E_{-k}$ and $|a_{vk}| = |a_{v-k}|$ for every eigenstate, considering an even N. Therefore, in the off-resonant two-level interaction regime, we trivially get $\Delta/J' = 0$ and so $C^{(i)} = 1$ provided $\omega_v = 0$ and g_v is small enough, so as to justify the two-level approximation [Eq. (6)].

Another very relevant aspect of nearest-neighbor off-diagonal disorder in tight-bindings models is the emergence of an anomalous mode at the very center of the band featuring a diverging localization length. Indeed, the density of states shows a logarithmic singularity in this region [49]. For odd values of N, we thus get a *fixed* energy level $E_{k'} = 0$ for every realization of disorder Thereby, this time we focus on the effective three-level scenario, Hamiltonian (10), with $\omega_s = \omega_r = E_{k'}$. Note that this regime can be also achieved for even N. The reason we chose to restrict the following discussion to odd N is partly to bypass the need to reset ω sample after sample in order to meet a given channel's normal mode around the center of the band.

Figure 3 shows the behavior of concurrence $C^{(ii)}$ with α. We note that uncorrelated disorder ($\alpha = 0$) already offers a reasonable amount of entanglement though it diminishes with increasing N. This is due to the finiteness of the system added by the unusual properties of the corresponding channel eigenstate at $E_{k'} = 0$ that acts as sort of a pseudo-delocalized state with a stretched exponential envelope [49]. For $N = 151$ and 201, we again spot a pronounced increase in the concurrence when $\alpha > 1$. This naturally comes out as a response to the emergence of delocalization around the center of the band. We shall, however, remark that the regime $1 < \alpha < 2$ does not actually provide *true* extended states [50], though the participation number increases quite considerably [51]. In this effective three-level (sender–channel–receiver resonant) scenario though, the outer entangling spins are being mediated *solely* by the anomalous eigenstate at $E_{k'} = 0$. We thus realize that this state is very sensitive to α in such a way that $\alpha > 2$ guarantees the necessary symmetry, $|\eta| \approx 1$, to support maximal entanglement between both parties. We must stress, however, that this behavior could have also been seen if we had set ω_s in resonance with some other nearby mode. In fact, although the anomalous eigenstate shows very peculiar features for uncorrelated structural disorder [49,50], the overall trend when $\alpha > 0$ is—similarly to what happens in the on-site disorder case—the appearance of delocalized states in the neighborhood of $E_{k'} = 0$, including the anomalous mode itself, with roughly the same localization length [35].

The major difference between both diagonal and off-diagonal disorder cases is how fast delocalization is built with α. This can be seen indirectly through the stabilization of the end-to-end concurrence by comparing Figs. 1 and 3. In order to further illustrate that, in Fig. 4 we show a typical (single) realization of the wavefunction (its squared modulus) corresponding to a given channel mode selected at $E_{k'} \approx 0$ for both kinds of disorder and $N = 201$. As expected, in the case of spin-coupling disorder (Fig. 4a), the wavefunction features a much larger localization length than the on-site disorder counterpart (Fig. 4b) already for $\alpha = 1$. When $\alpha = 2$, we note in Fig. 4a that the state shows fairly balanced overlaps $|a_{sk'}| = |\langle 1|E_{k'}\rangle|$ and $|a_{rk'}| = |\langle N|E_{k'}\rangle|$, which is crucial for having $|\eta| \approx 1$ [cf. Eq. (11)] and hence $C^{(ii)} \approx 1$. That explains the behavior seen in Fig. 3. On the other hand, the wavefunction in Fig. 4b when $\alpha = 2$ still features a reminiscent localized-like profile. Things get more alike only at higher values of α as seen in the bottom panels of Fig. 4 for $\alpha = 3$. At this point, note that $|a_{sk'}| \approx |a_{rk'}|$ for both types of disorder. While this is responsible for yielding very high concurrences (see Figs. 1 and 3), as long as we depend upon a single mode of the channel such as in the effective three-level regime [Eq. (10)] and this very state happens to be a suitable one, there is no need to worry about the rest of the spectrum, unlike in the two-level regime where the effective detuning between $|s\rangle$ and $|r\rangle$ is largely influenced by the modes lying around ω_v, weighted by $(E_k - \omega_v)^{-1}$ [see Eqs. (7) and (8)]. Still, in this case, one can achieve nearly maximal entanglement provided α is high enough, as seen in Figs. 1 and 2.

5.3 End-to-end concurrence and quantum state transfer

Last, we discuss the relationship between the end-to-end entanglement evaluated in the previous section and the prospects of performing high-fidelity QST protocols [2]. The standard quantifier to access the channels' capacity of transmitting an arbitrary qubit state is given by the so-called input-averaged fidelity $F(t) = 1/2 + f(t)\cos(\varphi)/3 + f(t)^2/6$, which in turn depends on the transition amplitude $f(t) = |\langle r|e^{-i\hat{H}t}|s\rangle|$ between the sender and receiver and its associate phase φ, though this one can generally be ignored by a convenient choice of the of the on-site potentials ($\cos\varphi \equiv 1$) [2]. Note that if the phase is completely randomized, the fidelity becomes the classical one $F = 2/3$.

Working out the eigenproblem for both Hamiltonians (6) and (10), we get, respectively,

$$f^{(i)}(t) \equiv C^{(i)} \left| \sin\left(\frac{\sqrt{\Delta^2 + 4J'^2}}{2} t \right) \right|, \tag{15}$$

$$f^{(ii)}(t) \equiv \frac{C^{(ii)}}{2} \left| \cos\left[\sqrt{(g_s a_{sk'})^2 + (g_r a_{rk'})^2}\, t \right] - 1 \right|. \tag{16}$$

Note that the transition amplitude for each scenario, (i) and (ii), is directly proportional to the corresponding concurrence, this quantity thus being a primary indicator of the transfer quality in weak-coupling models. Taking $g_s = g_r = g$, whenever $f(t)$

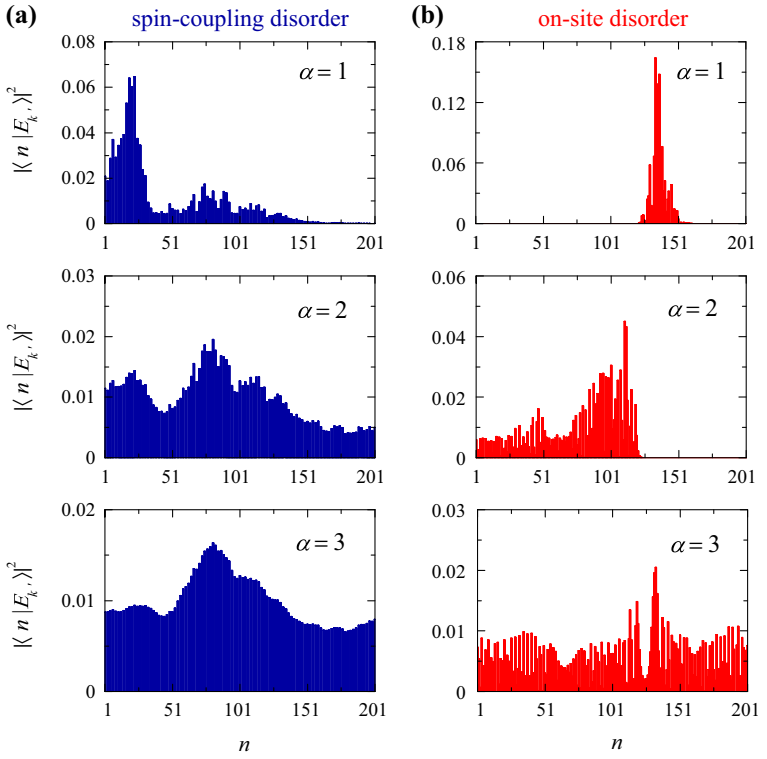

Fig. 4 Square modulus of the wavefunction $|\langle n|E_{k'}\rangle|^2$ versus n for several values of α for a single realization of **a** spin-coupling disorder and **b** on-site disorder. The corresponding eigenstate of the channel, $|E_{k'}\rangle$, was picked from the middle of the band, $E_{k'} \approx 0$ and the size of the chain was $N = 201$ (Color online)

reaches its maxima, that is at $\tau = \pi/\sqrt{\Delta^2 + 4J'^2} = \pi/\Omega$ for $f^{(i)}(\tau)$ and $\tau = \pi/(g\sqrt{a_{sk'}^2 + a_{rk'}^2})$ for $f^{(ii)}(\tau)$, the transition amplitude becomes the concurrence itself.

We must recall that all the above is valid once g is treated *perturbatively* in comparison with all the other coupling parameters. If that is not the case, we should expect the end-to-end concurrence to drop down due to the mixing between $|s\rangle$, $|r\rangle$ and the normal modes of the channel. In Fig. 5 we show the behavior of the end-to-end concurrence against α for several values of g for $N = 50$ (Fig. 5a) and $N = 51$ (Fig. 5b) (plus the sender and receiver), in the case of on-site and coupling disorder, respectively, now considering the full Hamiltonian, Eq. (1). For comparison, there we also show the curve (solid black line) obtained directly from the effective descriptions (previously shown in Figs. 1 and 3). Naturally, it fits very well with the plot corresponding to the lowest value of g in Fig. 5a and b. Still, despite the considerable weakening of entanglement upon increasing g, we note that the way the concurrence builds up with α remains the same.

Finally, note that the transfer time goes $\sim g^{-2}$ for the off-resonant regime and $\sim g^{-1}$ for the resonant case [6]. Since high fidelities outcomes requires very small

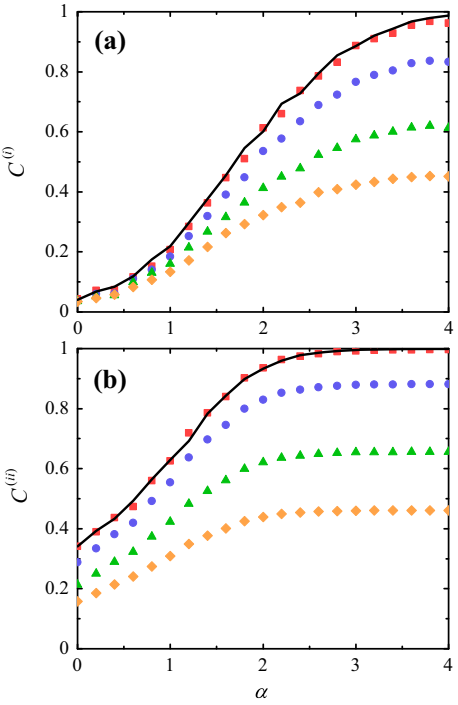

Fig. 5 End-to-end concurrences **a** $C^{(i)}$ and **b** $C^{(ii)}$ versus α averaged over 500 independent realizations of a **a** 50-site channel featuring on-site disorder and a **b** 51-site channel with spin-coupling disorder with fixed $\omega_r = \omega_s = 0$. The solid black curve corresponds to the solution obtained directly from the effective Hamiltonians, Eqs. (6) and (10), that is, without explicitly setting a value for g (cf. Figs 1, 3). Symbols depict the results from exact numerical diagonalization of the full Hamiltonian, Eq. (1) with $g = 0.01$ (red squares), 0.1 (blue spheres), 0.2 (green triangles), and 0.3 (yellow diamonds) in units of J ($4.5J$) in panel (**a**) [(**b**)]. In the case of on-site disorder (**a**), in each realization we chose the highest $C^{(i)}$ outcome among the states lying around the center of the band (due to the lack of particle–hole symmetry in the spectrum) and averaged it over all the samples (Color online)

values of g, weak-coupling models in general will demand longer operation times (especially in the off-resonant scenario) when compared to other schemes (cf. [30]), what could potentially damage the performance of the channel due to decoherence effects [52]. A possible way around is to bring the channel to operate in the ballistic regime by optimizing the outer couplings [9,53] in order to ease the fidelity-speed cost. The requirement for g shall also be relaxed by locally modifying a few coupling strengths in the channel [15] Still, weak-coupling configurations are very appealing for it offers great resilience against various forms of noise [28,54,55], as we have also showed here in the presence of correlated disorder.

6 Concluding remarks

We investigated the emergence of eigenstate entanglement between the two weakly coupled ends of a disordered linear XY spin-1/2 chain in two different interaction

regimes, namely when both outer spins are off-resonantly coupled to the channel and when they are put in narrow resonance with one of its natural modes. In both cases, we found that quantum channels presenting long-range correlated fluctuations is capable of mediating extremely high amounts of pairwise entanglement through long distances, thus embodying a robust platform for carrying out quantum communication tasks in the presence of imperfections. We also showed that spin-coupling strengths (structural) fluctuations are less detrimental than on-site disorder since the former assures particle–hole symmetry and induces the appearance of an eigenstate at the very center of the band showing ubiquitous localization properties.

One of the advantages of such a class of weakly coupled spin models offers is that the communicating parties only have access to the spectrum of the channel locally through the sites they are coupled to. Therefore, perfect spatial mirror symmetry can be put aside as long as a proper set of delocalized states are available in the spectrum, thus leading to an effective resonant coupling between both outer spins no matter their distance.

Acknowledgements This work was partially supported by CNPq (Grant No. 152722/2016-5), CAPES, FINEP, and FAPEAL (Brazilian agencies).

References

1. Nielsen, M.A., Chuang, I.L.: Quantum Computation and Quantum Information. Cambridge University Press, Cambridge (2000)
2. Bose, S.: Quantum communication through an unmodulated spin chain. Phys. Rev. Lett. **91**, 207901 (2003)
3. Christandl, M., Datta, N., Ekert, A., Landahl, A.J.: Perfect state transfer in quantum spin networks. Phys. Rev. Lett. **92**, 187902 (2004)
4. Plenio, M.B., Hartley, J., Eisert, J.: Dynamics and manipulation of entanglement in coupled harmonic systems with many degrees of freedom. New J. Phys. **6**, 36 (2004)
5. Wojcik, A., Luczak, T., Kurzynski, P., Grudka, A., Gdala, T., Bednarska, M.: Unmodulated spin chains as universal quantum wires. Phys. Rev. A **72**, 034303 (2005)
6. Wojcik, A., Luczak, T., Kurzynski, P., Grudka, A., Gdala, T., Bednarska, M.: Multiuser quantum communication networks. Phys. Rev. A **75**, 022330 (2007)
7. Li, Y., Shi, T., Chen, B., Song, Z., Sun, C.-P.: Quantum-state transmission via a spin ladder as a robust data bus. Phys. Rev. A **71**, 022301 (2005)
8. Huo, M.X., Li, Y., Song, Z., Sun, C.-P.: The peierls distorted chain as a quantum data bus for quantum state transfer. Europhys. Lett. **84**, 30004 (2008)
9. Apollaro, T.J.G., Banchi, L., Cuccoli, A., Vaia, R., Verrucchi, P.: 99%-Fidelity ballistic quantum-state transfer through long uniform channels. Phys. Rev. A **85**, 052319 (2012)
10. Salimi, S., Ghoraishipour, S., Sorouri, A.: Perfect state transfer via quantum probability theory. Quantum Inf. Process. **12**, 505 (2013)
11. Lorenzo, S., Apollaro, T.J.G., Paganelli, S., Palma, G.M., Plastina, F.: Transfer of arbitrary two-qubit states via a spin chain. Phys. Rev. A **91**, 042321 (2015)
12. Sandberg, M., Knill, E., Kapit, E., Vissers, M.R., Pappas, D.P.: Efficient quantum state transfer in an engineered chain of quantum bits. Quantum Inf. Process. **15**, 1213 (2016)
13. Almeida, G.M.A., Ciccarello, F., Apollaro, T.J.G., Souza, A.M.C.: Quantum-state transfer in staggered coupled-cavity arrays. Phys. Rev. A **93**, 032310 (2016)
14. Kempton, M., Lippner, G., Yau, S.-T.: Pretty good quantum state transfer in symmetric spin networks via magnetic field. Quantum Inf. Process. **16**, 210 (2017)
15. Almeida, G.M.A.: Interplay between speed and fidelity in quantum-state transfer protocols via effective Rabi dynamics. Phys. Rev. A **98**, 012334 (2018)

16. Amico, L., Osterloh, A., Plastina, F., Fazio, R., Palma, G.M.: Dynamics of entanglement in one-dimensional spin systems. Phys. Rev. A **69**, 022304 (2004)
17. Plastina, F., Apollaro, T.J.G.: Local control of entanglement in a spin chain. Phys. Rev. Lett. **99**, 177210 (2007)
18. Campos Venuti, L., Degli Esposti Boschi, C., Roncaglia, M.: Long-distance entanglement in spin systems. Phys. Rev. Lett. **96**, 247206 (2006)
19. Gualdi, G., Giampaolo, S.M., Illuminati, F.: Modular entanglement. Phys. Rev. Lett. **106**, 050501 (2011)
20. Estarellas, M.P., D'Amico, I., Spiller, T.P.: Robust quantum entanglement generation and generation-plus-storage protocols with spin chains. Phys. Rev. A **95**, 042335 (2017)
21. Almeida, G.M.A., de Moura, F.A.B.F., Apollaro, T.J.G., Lyra, M.L.: Disorder-assisted distribution of entanglement in XY spin chains. Phys. Rev. A **96**, 032315 (2017)
22. Bellec, M., Nikolopoulos, G.M., Tzortzakis, S.: Faithful communication hamiltonian in photonic lattices. Opt. Lett. **37**, 4504 (2012)
23. Perez-Leija, A., Keil, R., Kay, A., Moya-Cessa, H., Nolte, S., Kwek, L.-C., Rodríguez-Lara, B.M., Szameit, A., Christodoulides, D.N.: Coherent quantum transport in photonic lattices. Phys. Rev. A **87**, 012309 (2013)
24. De Chiara, G., Rossini, D., Montangero, S., Fazio, R.: From perfect to fractal transmission in spin chains. Phys. Rev. A **72**, 012323 (2005)
25. Burgarth, D., Bose, S.: Perfect quantum state transfer with randomly coupled quantum chains. New J. Phys. **7**, 135 (2005)
26. Tsomokos, D.I., Hartmann, M.J., Huelga, S.F., Plenio, M.B.: Entanglement dynamics in chains of qubits with noise and disorder. New J. Phys. **9**, 79 (2007)
27. Petrosyan, D., Nikolopoulos, G.M., Lambropoulos, P.: State transfer in static and dynamic spin chains with disorder. Phys. Rev. A **81**, 042307 (2010)
28. Yao, N.Y., Jiang, L., Gorshkov, A.V., Gong, Z.-X., Zhai, A., Duan, L.-M., Lukin, M.D.: Robust quantum state transfer in random unpolarized spin chains. Phys. Rev. Lett. **106**, 040505 (2011)
29. Zwick, A., Álvarez, G.A., Stolze, J., Osenda, O.: Robustness of spin-coupling distributions for perfect quantum state transfer. Phys. Rev. A **84**, 022311 (2011)
30. Zwick, A., Álvarez, G.A., Stolze, J., Osenda, O.: Spin chains for robust state transfer: modified boundary couplings versus completely engineered chains. Phys. Rev. A **85**, 012318 (2012)
31. Ashhab, S.: Quantum state transfer in a disordered one-dimensional lattice. Phys. Rev. A **92**, 062305 (2015)
32. Phillips, P., Wu, H.-L.: Localization and its absence: a new metallic state for conducting polymers. Science **252**, 1805 (1991)
33. de Moura, F.A.B.F., Lyra, M.L.: Delocalization in the 1d anderson model with long-range correlated disorder. Phys. Rev. Lett. **81**, 3735 (1998)
34. Domínguez-Adame, F., Malyshev, V.A., de Moura, F.A.B.F., Lyra, M.L.: Bloch-like oscillations in a one-dimensional lattice with long-range correlated disorder. Phys. Rev. Lett. **91**, 197402 (2003)
35. Lima, R.P.A., Lyra, M.L., Nascimento, E.M., de Jesus, A.D.: Magnon delocalization in ferromagnetic chains with long-range correlated disorder. Phys. Rev. B **65**, 104416 (2002)
36. de Moura, F.A.B.F., Coutinho-Filho, M.D., Raposo, E.P., Lyra, M.L.: Delocalization and spin-wave dynamics in ferromagnetic chains with long-range correlated random exchange. Phys. Rev. B **66**, 014418 (2002)
37. Montangero, S., Benenti, G., Fazio, R.: Dynamics of entanglement in quantum computers with imperfections. Phys. Rev. Lett. **91**, 187901 (2003)
38. Refael, G., Moore, J.E.: Criticality and entanglement in random quantum systems. J. Phys. A Math. Theor. **42**, 504010 (2009)
39. Binosi, D., De Chiara, G., Montangero, S., Recati, A.: Increasing entanglement through engineered disorder in the random ising chain. Phys. Rev. B **76**, 140405 (2007)
40. Rodriguez-Laguna, J., Santalla, S.N., Ramirez, G., Sierra, G.: Entanglement in correlated random spin chains, rna folding and kinetic roughening. New J. Phys. **18**, 073025 (2016)
41. Getelina, J.C., Alcaraz, F.C., Hoyos, J.A.: Entanglement properties of correlated random spin chains and similarities with conformally invariant systems. Phys. Rev. B **93**, 045136 (2016)
42. Giampaolo, S.M., Illuminati, F.: Long-distance entanglement in many-body atomic and optical systems. New J. Phys. **12**, 025019 (2010)

43. Sahling, S., Remenyi, G., Monceau, P., Saligrama, V., Marin, C., Revcolevschi, A., Regnault, L.P., Raymond, S., Lorenzo, J.E.: Experimental realization of long-distance entanglement between spins in antiferromagnetic quantum spin chains. Nat. Phys. **11**, 255 (2015)
44. Santos, L.F., Rigolin, G.: Effects of the interplay between interaction and disorder in bipartite entanglement. Phys. Rev. A **71**, 032321 (2005)
45. Paczuski, M., Maslov, S., Bak, P.: Avalanche dynamics in evolution, growth, and depinning models. Phys. Rev. E **53**, 414 (1996)
46. Feder, J.: Fractals. Plenum Press, New York (1988)
47. Wootters, W.K.: Entanglement of formation of an arbitrary state of two qubits. Phys. Rev. Lett. **80**, 2245 (1998)
48. Anderson, P.W.: Absence of diffusion in certain random lattices. Phys. Rev. **109**, 1492 (1958)
49. Inui, M., Trugman, S.A., Abrahams, E.: Unusual properties of midband states in systems with off-diagonal disorder. Phys. Rev. B **49**, 3190 (1994)
50. Cheraghchi, H., Fazeli, S.M., Esfarjani, K.: Localization-delocalization transition in a one one-dimensional system with long-range correlated off-diagonal disorder. Phys. Rev. B **72**, 174207 (2005)
51. Assuncao, T.F., Lyra, M.L., de Moura, F.A.B.F., Domínguez-Adame, F.: Coherent electronic dynamics and absorption spectra in an one-dimensional model with long-range correlated off-diagonal disorder. Phys. Lett. A **375**, 1048 (2011)
52. Cai, J.-M., Zhou, J.-M., Guo, G.-C.: Decoherence effects on the quantum spin channels. Phys. Rev. A **74**, 022328 (2006)
53. Banchi, L., Apollaro, T.J.G., Cuccoli, A., Vaia, R., Verrucchi, P.: Long quantum channels for high-quality entanglement transfer. New J. Phys. **13**, 123006 (2011)
54. Zwick, A., Álvarez, G.A., Bensky, G., Kurizki, G.: Optimized dynamical control of state transfer through noisy spin chains. New J. Phys. **16**, 065021 (2014)
55. Qin, W., Wang, C., Zhang, X.: Protected quantum-state transfer in decoherence-free subspaces. Phys. Rev. A **91**, 042303 (2015)